Visakhapatnam Chapter

*Proceedings of Indian Geotechnical Conference 2020*
*December 17-19, 2020, Andhra University, Visakhapatnam*

# Analysis of Shotcrete Lining and Estimation of Support Pressure of Sardar Sarovar Underground Powerhouse Cavern

Narendra Kumar Samadhiya

Department of Civil Engineering, Indian Institute of Technology Roorkee, India, narendra.samadhiya@ce.iitr.ac.in

**Abstract.** The present paper deals with the finite element analysis of shotcrete lining of Sardar Sarovar project cavern intercepted by a shear zone. The shotcrete has been modelled using a single layer of 20-noded isoparametric brick element. A layer of joint elements has been added above the layer of brick elements to simulate the influence of surrounding rock mass. Following the concept of the substructure technique, the displacements obtained from the analysis of the cavern have been applied on to the outer surface of the joint elements (surface other than that in contact with the shotcrete) in order to obtain the displacements, support pressure and the stresses in the shotcrete. The support pressures obtained from numerical analysis have been compared with those obtained on the basis of conventional approaches. The long term support pressures computed in the present study are in good agreement with those obtained using Norwegian Geotechnical Institute criterion even near the shear zone. However, wall support pressures away from the shear zone are negligible due to lower stiffness of shotcrete in the horizontal direction.

**Key words:** Shotcrete, Lining, Support pressure

## 1 Introduction

Shotcrete is being used now a days as permanent and temporary support systems in combination with systematic rock reinforcement by bolts/anchors in underground excavations. The total thickness of shotcrete is usually kept in the range of 50 mm to 200 mm. It is applied in layers, each layer having a thickness in the range of 25 to 40 mm. The layer thickness in excess of 40 mm requires special mix design to minimise rebound losses. When multiple layers are used, a welded wire mesh or expanded metal mesh is usually provided between layers. The Sardar Sarovar Powerhouse (SSP) cavern has been supported by rock bolts and shotcreting with wire mesh. Pattern bolting used tensioned, expansion shell type 25 mm dia. rock bolts, 6 m long at 1.75 m c/c staggered in the roof arch. The bolts were pretensioned to 140 kN load and grouted [1]. Two layers of shotcrete, each of 38 mm thick were provided with welded wire mesh. The overall thickness of shotcrete including the wire mesh was 85 mm.

Attempts have been made in the past by many research workers to estimate the support pressures [2-9]. The most widely accepted contribution is based on the Q system [10].

The finite element analysis of shotcrete lining of SSP cavern has been presented in the paper. The finite element analysis which has been carried out to study the influence of shotcrete lining is a linear analysis only. The support pressures obtained from numerical analysis have also been compared with those obtained on the basis of conventional approaches.

## 2 Sardar Sarovar Powerhouse (SSP) Cavern

Sardar Sarovar project is a World Bank aided multipurpose river valley project constructed on river Narmada and is situated at Kevadia village in of Gujarat state in India. The project includes a 138.68m high and 1210 m long concrete gravity dam. The underground powerhouse cavern, aligned N $10^o$ E (i.e. parallel to the main dam), is a large cavern of 23 m width x 210 m length x 58 m height. The cavern is located at about 30 to 65 m below the average ground level and is surrounded by lava flows of dense, porphyritic and amygdular varieties. Flows are separated by discontinuous bands of agglomerates and have been intruded by two dolerite dykes ranging in thickness from 40 to 55 m. One such dyke, which cuts the alignment from chainage 1448 m to 1492.5 m at the cavern axis, is aligned in N $70^0$ E - S $70^0$ W direction and dips at $60^0$ - $65^0$ towards the river side [11]. Both contacts of this dyke with adjoining basalt flows are sheared. The first sheared contact (shear zone A) is thin and does not intersect the cavern, whereas the second sheared contact (shear zone B) is 1 - 2m wide and intersects the cavern roof at chainage 1492.5 m (Fig. 1.)

Another dyke, traversing the alignment between chainage 1698 m and 1753 m, is 55 m wide and trends in N $75^0$ E - S $75^0$ W direction with vertical disposition. The contact of this dyke at chainage 1698 m with the adjacent basalts is comparatively tight, though some calcification has been observed at the contact. These two dykes join and form a 25 m thick sill near the turbine level. This sill has fused contacts with the basalts. Agglomerate bands are present at the interfaces of different lava flows. In all three such agglomerate layers are noticed surrounding the powerhouse cavern. Their contacts with the overlying and underlying basalt flows vary from sharp to gradational.

Some of the important chainages (at cavern axis) with reference to Fig. 1 are as follows:

i) Ch.1438.0 m intersection of shear zone ‘A’,
ii) Ch.1468.0 m the southern face of cavern,
iii) Ch.1492.5 m intersection of shear zone ‘B’,
iv) Ch.1628.0 m the start of bench towards southern end,
v) Ch.1678.0 m the northern face of cavern,
vi) Ch.1708.0 m the start of vertical dolerite dyke, 55 m wide.

A longitudinal section of the powerhouse cavern excavated through jointed basalts, jointed dolerites and shear zones is shown in Fig. 1.

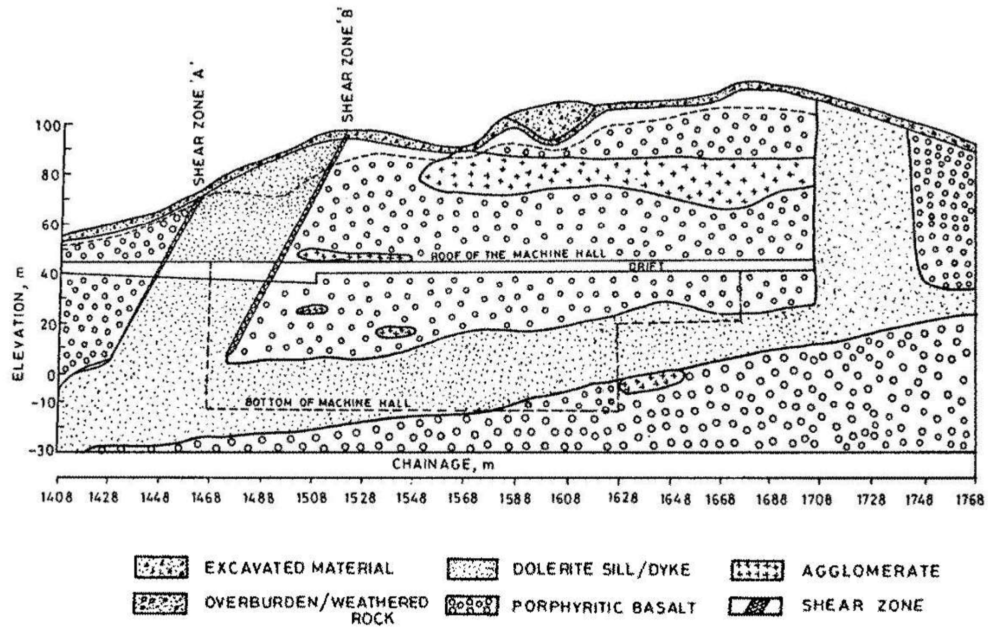


**Fig. 1.** Longitudinal Section of the Sardar Sarovar powerhouse cavern (Verman et al.1993).

The rock mass quality of various litho units encountered in the powerhouse cavern is evaluated on the basis of lithology, joint pattern and structural discontinuities [1]. In all, the rock mass encountered in the cavern may be classified into three categories:

i) Jointed basalts - moderately jointed, massive to blocky,
ii) Jointed dolerites - moderately jointed, hard dolerite dykes,
iii) Shear zone - sheared and fractured zone present near the contact of the dolerite dyke and adjacent basalts.

The study of joints in the rock mass exposed in the enlarged drift has been made for the spacing, orientation, aperture, infilling, nature of wall rock etc. [12]. The results of the joint analysis have been summarized as in Table 1.

A three dimensional view of finite element mesh with cavern has been presented in Fig. 2 for visualisation of the problem.

The analysis of Sardar Sarovar powerhouse cavern was performed with the actual joint data (Table 1) and shear zones. A general purpose software ASRAM (Analysis of Stresses in Anisotropic Rock Masses) was developed for the 3-dimensional analysis of rock engineering problems with capability to simulate most of the problems associated with the geological discontinuities, like shear zones and fault zones [13].

**Table 1.** Material Properties of Anisotropic Rock Mass with Shear Zones [18]

| Material | Modulus of Deformation of rock material | Poisson's ratio | Number of Joint sets | Normal stiffness | | Shear stiffness |
|---|---|---|---|---|---|---|
| | $E_r$, GPa | $\nu_r$ | n | $k_{nl}$, GPa/m | $k_{nu}$, GPa/m | $K_s$, GPa/m |
| Basalts | 23.0 | 0.2 | 3 | 150.0 | 45.0 | 15.0 |
| Dolerites | 19.0 | 0.2 | 3 | 90.0 | 27.0 | 9.0 |
| Basalt & dolerite affected by shear zone | 23.0 | 0.2 | 3 | 20.0 | 14.0 | 2.0 |
| Agglomerates | 15.0 | 0.2 | -- | -- | -- | -- |
| Shear zone material | 15.0 | 0.25 | 1 | 15.0 | 10.5 | 1.5 |
| Joint element | | | | | | |
| Rock -shear zone | | | | 5.0 | | 2.0 |
| Rock - rock | | | | 30.0 | | 10.0 |

Note: $k_{nl}$ and $k_{nu}$ are normal stiffnesses of rock joints under loading and unloading respectively.

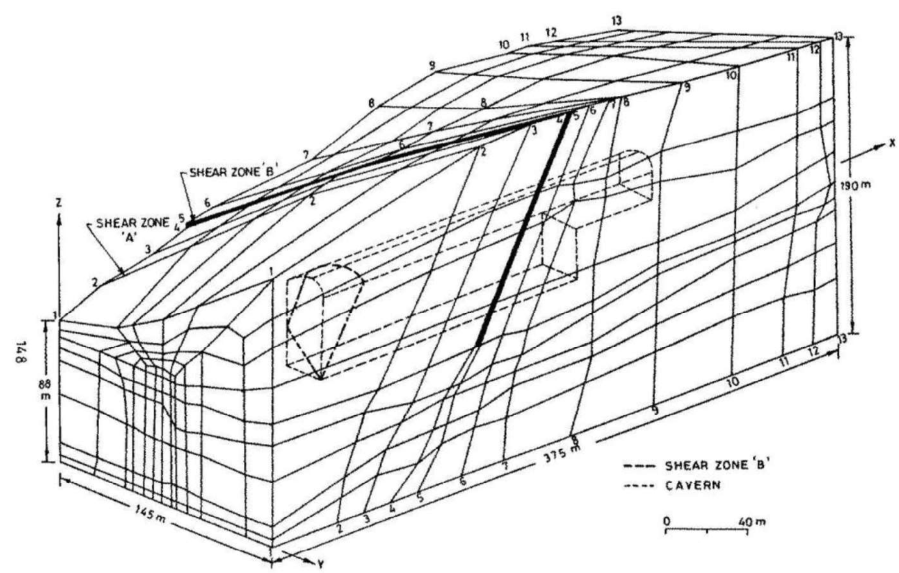


**Fig. 2.** Three dimensional view of finite element mesh of Sardar Sarovar powerhouse cavern

A detailed description on the elastic constitutive equations for the overall behaviour of rockmass based on the constitutive characteristics of intact rock and rock joints including their spacing,orientation and roughness has already been presented [14, 15].

A generalised formulation of a three dimensional joint/interface element to account for dilatancy, roughness and undulating surface of discontinuities has already been presented [16].

The in-situ horizontal major principal stress, along the longitudinal axis of the cavern and the intermediate principal stress across the cavern, were found to be 2.8 and 1.3times the vertical stress, respectively [17].

The material properties used for characterising the anisotropic continuum were obtained using the technique of back-analysis of the observed displacements for 39 m deep excavation of SSP cavern. In this case, actual joint sets with their respective orientations have been accounted for along with stress dependent moduli and stiffnesses of the joints. The final values of mechanical properties used are presented in Table 1.

The displacement behaviour and stress distribution around the cavern based on the above analysis have already been presented [18]. The displacements so obtained have been used as boundary conditions for the analysis of shotcrete lining.

## 3 Modelling of Shotcrete

Initially efforts were made to consider the thin shotcrete lining along with the analysis of the cavern. However, severe difficulty was faced in ensuring proper aspect ratio of the curved isoparametric elements of shotcrete in the roof. It was realised that number of elements in the cavern and shotcrete would increase many times for combined analysis, which was not practicable in the proposed study. Hence, it was necessary to analyse shotcrete lining by the method of sub structuring. In this technique, a large structure, which is difficult to be analysed as a whole, is divided into blocks which are analysed separately. The sequence of analysis for various parts is based on the influence of one part on the other. In the present case, the SSP cavern is divided into two parts viz. (i) Powerhouse Cavern and (ii) Shotcrete. The stiffness of shotcrete is negligible in comparison to that of the surrounding rock mass. If the cavern is analysed without shotcrete, the results are likely to remain same. However, the behaviour of shotcrete is totally dependent on the displacements of the cavern. The displacements derived from the analysis of the cavern have been applied on to the outer surface of the joint elements (surface other than that in contact with the shotcrete) to obtain the displacements, support pressure and the stresses in the shotcrete.

The effect of rock bolts has not been considered in the analysis of the cavern. Firstly, because the stiffness of the rock bolts is negligible compared to the stiffness of the rock mass and secondly pretension of rock bolts distributed over the excavated surface [140/(1.75 x 1.75) $kN/m^2$ ] is too small compared to the in-situ stresses.

The shotcrete lining of Sardar Sarovar Powerhouse (SSP) cavern has been modelled using a single layer of 20-noded isoparametric brick element. The portion of shotcrete modelled includes that in the side walls, crown and on southern face. The southern face has been included due to the presence of the shear zone 'B'. The portion of shotcrete on the faces of the benches has been ignored because it is far away from the shear zone 'B'. A layer of joint elements has been added above the layer of brick elements to simulate the influence of surrounding rock mass.

As per the requirements of the substructure technique, the Finite Element mesh of both the parts i.e. cavern and shotcrete, should have nodal correspondences so that the displacements obtained from analysis of the first part may be applied as boundary displacements, while analysing the second part. To fulfil this condition, internal surface of the powerhouse cavern has been developed. All the nodes lying on the excavated face of the cavern have also been marked on it. To prepare the mesh for shotcrete, new nodes have been added within the existing nodes to have a much finer mesh. Thus, developed surface used for shotcrete analysis is shown in Fig. 3.

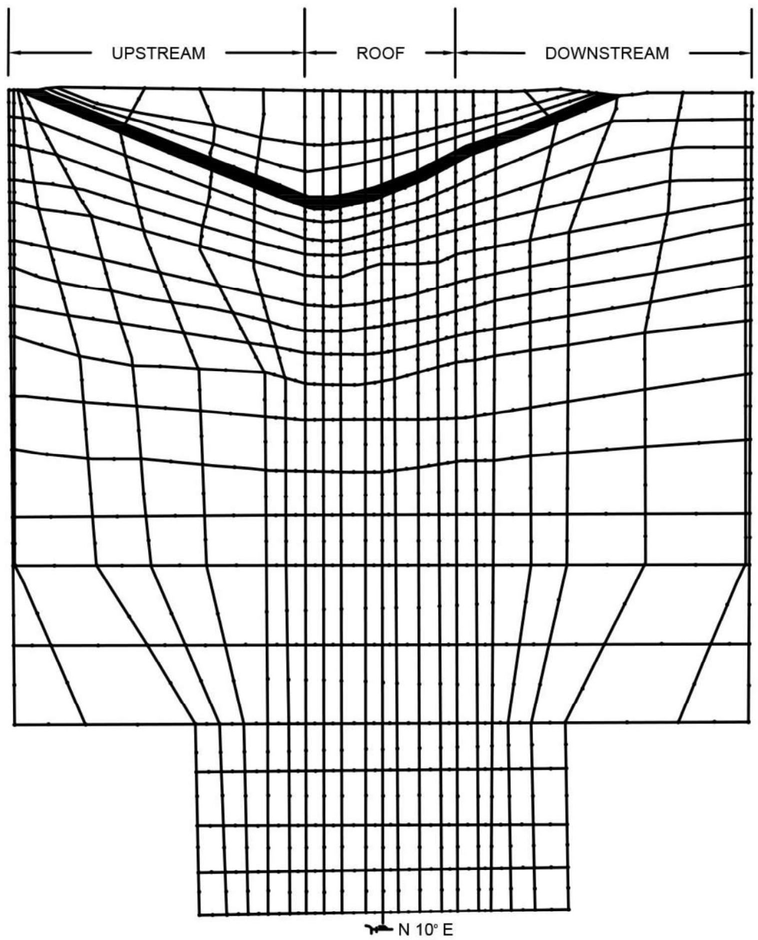


**Fig. 3.** Developed internal surface of SSP

This refined mesh forms the top face of the joint element layer. As the joint element has got zero thickness this also forms the common surface between the joint element and the shotcrete. The co-ordinates of the inner surface of the shotcrete have been obtained by applying due corrections to the previously obtained co-ordinates of the outer surface for the thickness (85 mm) of shotcrete. A typical cross section of the shotcrete has been presented in Fig.4.

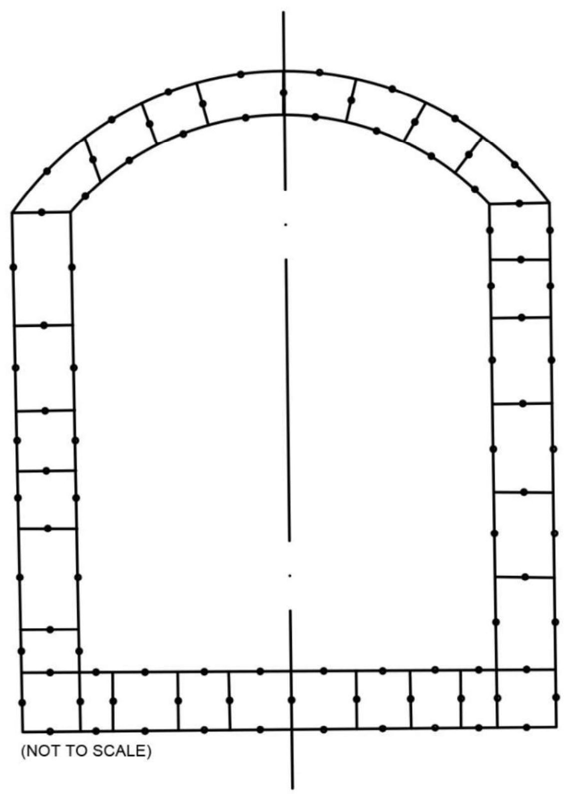


**Fig. 4.** Typical cross section of the shotcrete lining

The boundary conditions have been imposed by assigning the displacements (obtained from the analysis of powerhouse cavern for anisotropic rock mass model) at corresponding nodes lying on the outer surface of the joint element. The elements in shotcrete layer lying at side wall-floor junction have also been subjected to prescribed displacements equal to the displacements obtained from the analysis of the cavern at the same point.

The finite element analysis whichhas been carried out to study the influence of shotcrete lining is a linear analysis only.

A summary of the mesh has been presented in Table 2.

**Table 2.** Summary of Finite Element Mesh for Shotcrete

| Elements | |
|---|---|
| Total | 980 |
| 20 Noded (Brick) | 490 |
| 16 Noded (joint) | 490 |
| Nodes | |
| Total | 5114 |
| Boundary | 1557 |

**Material Properties:** For shotcrete, typical values of the material properties [19] have been assumed which are presented in Table 3.

**Table 3.** Material Properties for Shotcrete [19]

| S. No. | Parameter | Unit | Value |
|---|---|---|---|
| 1. | Modulus of Deformation ($E_d$) | $kN/m^2$ | $0.25 \times 10^8$ |
| 2. | Poisson's Ratio (ν) | - | 0.15 |
| 3. | Compressive Strength | $kN/m^2$ | 35000 |
| 4. | Permissible Stress | | |
| | a) Compression | $kN/m^2$ | $0.9 \times 10^4$ |
| | b) Tension | $kN/m^2$ | $0.3 \times 10^4$ |
| | c) Flexure | $kN/m^2$ | $0.2 \times 10^4$ |
| | d) Shear | $kN/m^2$ | $0.4 \times 10^4$ |

In this analysis, the joint element has been used to simulate the influence of surrounding rock mass. Each joint element acts as a spring in the direction normal to the surface of the shotcrete, the stiffness of which has been determined as-

$k_n$= pressure/displacement

= normal in-situ stress / displacement due to release of in-situ stress

Here, pressure has been used instead of load because $k_n$ represents pressure or stress responsible for causing a unit displacement. Since the in-situ stress normal to the excavated face has been released due to excavation, therefore $k_n$ can easily be determined by dividing the in-situ stress at any point by the displacement at that point. However, as both the displacements and in-situ stress vary from point to point, a constant value of $k_n$ cannot be used for all the joint elements. Therefore, entire shotcrete surface has been divided in to 13 regions shown in Fig.5.

The values of $k_n$ obtained for all these regions have been presented in Table 4. For determining the value of $k_n$ for a particular region, $k_n$ was calculated at all the nodes within that region and then an average value was adopted. Since the shotcrete was expected to have good bonding with the rock mass, no slip has been allowed between the two and therefore shear stiffnesses $k_{s1}$ and $k_{s2}$ have been equated to the normal stiffness, $k_n$

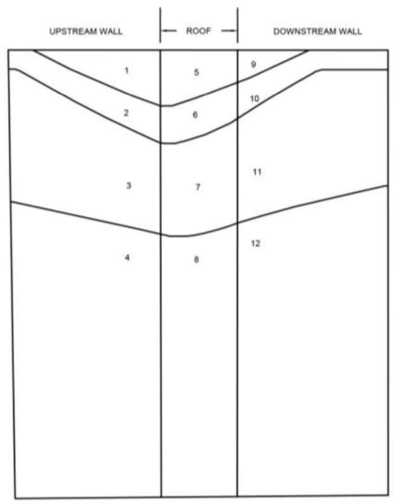


**Fig. 5.** Material regions for the shotcrete lining

# 4 Discussion of Results

## 4.1 Displacements

The displacements of the cavern with and without shotcrete layer have been plotted in Figs 6 and 7 for side walls. The displacements of side walls have been plotted at the mid height. The displacements of the cavern without shotcrete have also been shown along with. The shotcrete, in general, reduces the displacements only marginally. The effect is more pronounced at the crown whereas at the side walls, the reduction is small.

**Table 4.** Normal Stiffness ($k_n$) for Joint Elements

| S. No. | Region | $k_n$ x $10^4$kN/m$^3$ |
|---|---|---|
| | Up stream wall | |
| 1 | Near shear zone towards south | 30.0 |
| 2 | At and adjacent to shear zone | 15.0 |
| 3 | Near shear zone toward north | 12.0 |
| 4 | Away from shear zone | 26.0 |
| | Crown | |
| 5 | Near shear zone toward south | 33.0 |
| 6 | At and adjacent to shear zone | 20.0 |
| 7 | Near shear zone towards north | 35.0 |
| 8 | Away from shear zone | 65.0 |

| | | |
|---|---|---|
| | Down stream wall | |
| 9 | Near shear zone towards south | 40.0 |
| 10 | At and adjacent to shear zone | 22.0 |
| 11 | Near shear zone towards north | 15.0 |
| 12 | Away from shear zone | 33.0 |
| 13 | Southern face | 45.0 |

It can be seen in Fig. 8 that the kink observed in the displacement at the location of shear zone has disappeared due to shotcrete. However, very high shear stresses are likely to develop in shotcrete lining under such conditions. This was also confirmed by the appearance of cracks in shotcrete lining which have appeared in the shear zone area in the cavern [20].

### 4.2 Stresses in shotcrete

Table 5 gives maximum hoop, bending and shear stresses at a few typical locations. The variation of hoop stress and the bending stress has shown that the bending stresses are negligible in comparison to the hoop stress. This suggests that the membrane action is predominant over the bending action. This is in order as the shotcrete is very thin. However, high bending stresses were observed in shotcrete near the southern face in the lower portion of the upstream wall. These may be due to intersection of shear zone with upstream wall in this area. The hoop stresses were very high and almost equal throughout the width of the roof arch. In the side walls shotcrete, the hoop stresses are negligible at middle height, whereas these are relatively high near the springing level and wall-floor junctions.

A nearly constant magnitude of stress in the roof of cavern also suggests the membrane action in shotcrete lining. Hoop stresses in the roof lining are relatively higher at chainage 1493.0 m and in its vicinity on either side due to the presence of shear zone 'B'.

Conventionally, the shotcrete is checked against shear stresses in the roof lining. High shear stresses have been observed in shotcrete lining in the vicinity of the shear zone B. It has also been observed that distance between the two peaks of shear stress is around 0.67 times the semi-circular span of the opening. This distance can also empirically be deduced [21] as,

Distance between two peaks of shear stresses $= 0.55[(100 x t_{sc})^{0.05}] \times B$ (1)

where, $t_{sc}$ = shotcrete thickness in m,

B = width of cavern

For a shotcrete thickness of 85 mm, i.e., 0.085 m, this distance between two peaks of shear stresses works out to be 0.61 x B which compares very well with the actual average distance of 0.67 x B.

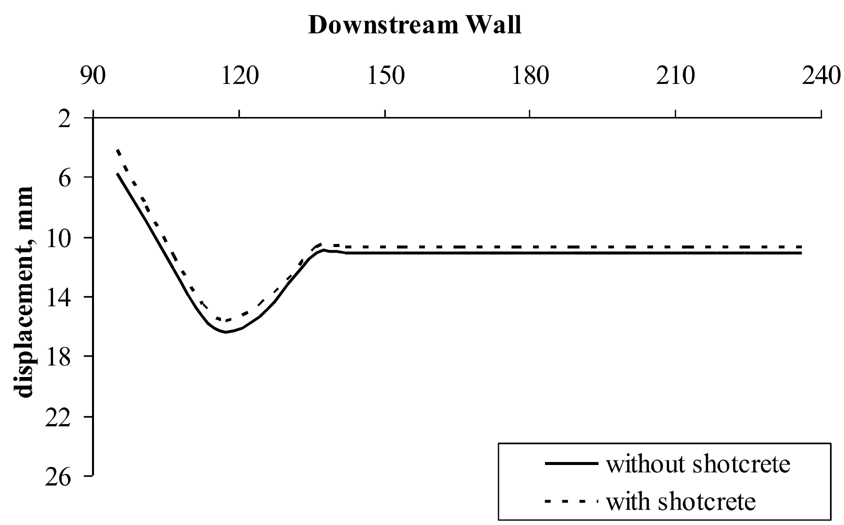


**Fig. 6.** Displacement of the downstream wall

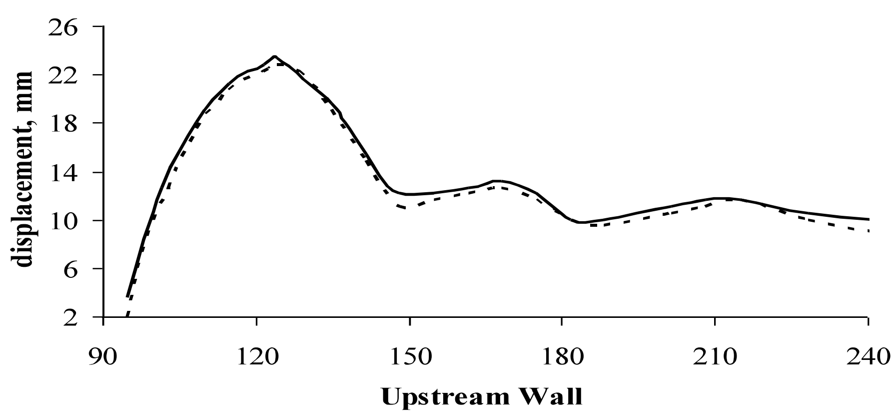


**Fig. 7.** Displacement of the upstream wall

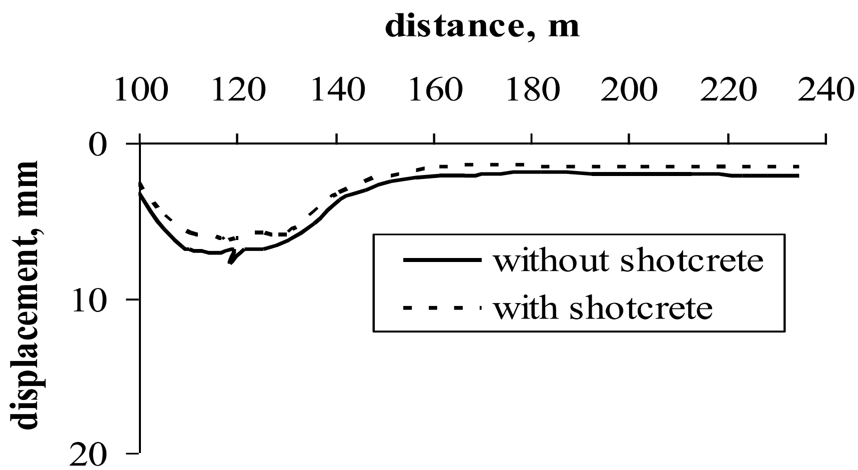


**Fig. 8.** Displacement of the crown

Maximum shear stresses in the roof have been presented for some typical locations in Table 5. On comparing the permissible stresses (Table 3) with induced stresses in shotcrete (Table 5), it can be inferred that the induced hoop and shear stresses are much higher in the vicinity of shear zone 'B' than the permissible stresses in shotcrete lining which can cause in cracking of shotcrete in the shear zone area. The lining, therefore, requires additional measures from safety considerations.

**Table 5.** Maximum Stresses in Shotcrete Lining at Roof

| Location Chainage | Hoop Stress[1] (kN/m$^2$) | Bending Stress[2] (kN/m$^2$) | Shear Stress (kN/m$^2$) |
|---|---|---|---|
| Roof Arch | | | |
| 1473.0 m | 11910 | -180 | 5100 |
| 1483.0 m | 18660 | -260 | 8700 |
| 1493.0 m | 22550 | -500 | 9600 |
| 1503.0 m | 22310 | -600 | 10500 |
| 1523.0 m | 12890 | -460 | 7500 |
| 1553.0 m | 11140 | -500 | 7550 |
| Safe Values | 9000 | -2000 | 4000 |

1: Compression (+); 2: Compression on inside surface (+)

### 4.3 Support pressures

An additional advantage of providing the joint elements over the shotcrete lining in this analysis is that the normal stresses on the joint element will directly provide the support pressures exerted by rock mass on the shotcrete lining. The variation of normal contact stress i.e. support pressure along the crown axis (cavern axis) has been depicted in Fig. 9.

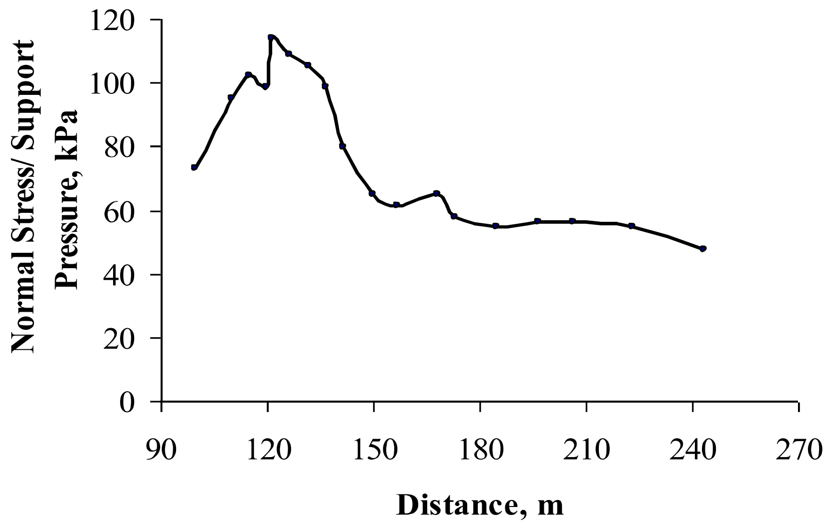


**Fig. 9.** Variation of normal contact Stress (Support pressure) along the crown axis

The support pressures are high in the vicinity of shear zone (75 kN /m2 - 115 kN/m2) whereas support pressures reduce to 50 - 65 kN/m2 away from the shear zone. The higher support pressures in the vicinity of shear zone may be due to the presence of weak rock mass and are corroborated by the corresponding high displacements (Fig. 8).

The pressures in the roof are relatively high towards the upstream wall side which may be due to higher overburden. The pressures in the side walls are high only near the springing levels whereas for major part of the wall height, the pressures are negligible. Negative wall support pressures have been observed near the shear zone area, which may lead to detachment of shotcrete from the side walls.

The high support pressures at crown may essentially be due to the geometric stiffness of the shotcrete (arch shape) at roof. However, as the walls are flat, they are unable to impart geometrical stiffness to the shotcrete. In addition to this, the shotcrete being thin enough (85 mm only), its own stiffness is also negligible. The combined effect may be responsible for low support pressures in side walls.

As discussed earlier, the roof support pressures are calculated using method (NGI Criterion) [10] as follows:

$$P_{roof} = \frac{200}{J_r} Q^{-\frac{1}{3}} \text{ kN/m}^2 \qquad (2)$$

where, Q = Barton's rock mass quality, and
$J_r$ = Joint roughness coefficient.

A method has been developed at Norwegian Geotechnical Institute (NGI) for assessing the support requirements using the Q - system for rock masses affected by shear zones. The use of mean value of Q, for the rockmass around the weak zone, has been advocated [22, 23] while using Eq. 2. The mean value of Q can be determined using the Eq. 3 as,

$$\log Q_m = \frac{b \times \log Q_{wz} + \log Q_{sr}}{b+1} \tag{3}$$

The author of the paper suggests that mean value of joint roughness coefficient, $J_{rm}$, should be estimated similarly as follows:

$$J_{rm} = \frac{b \times J_{rwz} + J_{rsr}}{b+1} \tag{4}$$

where
$Q_m$ = Mean value of Q
$Q_{wz}$ = Q value of weak zone
$Q_{sr}$= Q value of surrounding rock
b = thickness of the weak zone in m.
$J_{rm}$ = Mean value of $J_r$
$J_{rwz}$ = $J_r$ of the weak zone
$J_{rsr}$ = $J_r$ of surrounding rock

These values of Q and Jr should be substituted in Eq. 2. The estimated values of support pressures along with those obtained in the present study have been presented in Table 6.

**Table 6.** Estimated Values of Q and Long Term Roof Support Pressure

| Rock Mass Category | RQD [12] | $J_n$ [12] | $J_r$ [12] | $J_a$ [12] | $J_w$ [12] | SRF | Q | Long Term Roof Support Pressure (kPa) ($P_{roof}$) | | |
|---|---|---|---|---|---|---|---|---|---|---|
| | | | | | | | | NGI [10] | Present Study FEM | Typical Range [24] |
| Jointed Basalt | 55 | 12 | 1.5 $J_{rsr}$ | 0.75 | 1.0 | 1.0 | 9.16 $Q_{sr}$ | 64 | 55 | 50-108 |
| Jointed Dolerite | 65 | 12 | 1.5 | 0.75 | 1.0 | 1.0 | 10.88 | 60 | 84 | 47-102 |
| Shear Zone (b = 2m) | 25 | 2 | 1.0 $J_{rwz}$ | 4.00 | 1.0 | 2.5 | 1.25 $Q_{wz}$ | 186 | 110 | 107-218 |
| Mean Values Near Shear Zone | - | - | 1.17 $J_m$ | 2.90 | - | - | 2.4 $Q_m$ | 128 | 110 | 83-177 |

It is encouraging to note that the values of long term support pressures obtained in the present study are within the range of pressures predicted by Barton [24]. The values estimated by NGI criterion [10] are also comparable to the values obtained in the present study in jointed basalts and dolerites. However, at shear zone the support pressure predicted by NGI criterion is much higher (1.7 times) than that obtained in the present study (Table 6). However, when the mean values of Q [22] and $J_r$ are used, the support pressure near shear zone area has been found to be comparable to that obtained in the present study (Table 6).

The capacity of the roof supports, provided in the form of rock bolts and shotcrete lining, is 88 kN/m$^2$ [11]. It may be noted that the support pressures at the shear zones are of the order of 110 kN/m$^2$(obtained in the present study) exceeds the ultimate capacity of the support system and therefore cracking is likely to occur in the shear zone area. In fact cracking was indeed observed in the areas near shear zone and additional measures were suggested [20]. The use of 10 m long full column grouted rock bolts at 1.6 m x 1.6 m grid against 6 m long rock bolts at 1.75 m x 1.75 m grid installed in the cavern was also suggested [25].

The wall support pressure [10] is obtained as follows:

$$P_{wall} = \frac{200}{J_r}(Q_w)^{-\frac{1}{3}} \quad \text{kN/m}^2 \tag{4}$$

where $Q_w$ is the rock mass quality of the wall which is 2.5 x Q in the case of SSP cavern. As such the wall support pressures will be 0.74 times the long term roof pressures. It has been observed that the wall support pressures are negligible away from the shear zone as the horizontal stiffness of the shotcrete is low compared to the vertical stiffness of the shotcrete in arched roof. The average wall support pressure near shear zone is about 50 kN/m$^2$ against 90 kN/m$^2$ in the roof at chainage 1488.0 m. Thus the ratio between wall and roof support pressures is found to be about 0.5 against 0.74 near shear zone [10]. The predicted wall support pressures away from the shear zone are 0.06 - 0.11 times the roof support pressures.

## 5 Conclusions

The analysis of the Sardar Sarovar powerhouse cavern has been carried out along with the shotcrete lining. This study leads to following conclusions:

1. Shotcrete lining behaves essentially like a membrane.
2. The stresses in shotcrete are higher than the permissible stresses especially near the shear zone area.
3. The influence of shotcrete is negligible as far as the displacement behaviour of the cavern is concerned because of it's very low stiffness.
4. The empirical correlation for obtaining the distance between peak shear stress in shotcrete [21] has been found to be in good agreement with the results obtained in the present study.
5. The equation for mean value of joint roughness coefficient, $J_{rm}$, has been suggested.

6. The long term support pressures computed in the present study are in good agreement with those obtained using NGI criterion [10] even near the shear zone. However, wall support pressures away from the shear zone are negligible due to lower stiffness of shotcrete in the horizontal direction.
7. Failure of the support system in and around shear zone was indicated both in the present study and recommendations of CSIR-CIMFR Dhanbad [25] based on the empirical classifications.

## References


1. Chandra, P.: Problems encountered during the construction of powerhouse cavern and access tunnel excavations in Deccan trap at Sardar sarovar (Narmada) project, district Bharauch, Gujarat. Journal of Engineering Geology XXI(1 & 2), 99-106 (1992).
2. Cording, E.J., Henderson Jr. A.J., Deer D.V.: Rock engineering for underground caverns. In: Proceeding symposium on underground rock chambers, pp. 567-600, Phoenix Arizona, (1971).
3. Army Corps of Engineers: Engineering and design; rock reinforcement, engineers. Manual EM 1110 - 1 - 2907, Office of the Chief of Engineers, Washington D.C. 20314 (1980).
4. Yavuz, H.: Support pressure estimation for circular and non-circular openings based on a parametric numerical modelling study. Journal of the South African Institute of Mining and Metallurgy 106 (2),129-139,(2006).
5. Scussel, D., Chandra, S.: A new approach to obtain tunnel support pressure for polyaxial state of stress. Tunnelling and Underground Space Technology 36,80-88 (2013).
6. Prasad, V.V.R., Dwivedi, R.D., Swarup, A.: Determination of support pressure for tunnels and caverns using block theory. Tunnelling and Underground Space Technology 37,55-61(2013).
7. Naithani, A.K., Singh, L.G., Jain, P.: Rock mass characterization and support design for underground additional surge pool cavern—a case study, India. Geomaterials 7,64-82. https://doi.org/10.4236/gm.2017.72006 (2017)
8. Kong, X.X., Liu, Q.S., Zhang, Q.B.: A method to estimate the pressure arch formation above underground excavation in rock mass. Tunnelling and Underground Space Technology 71:382–390(2018).
9. Hongjie, Gao, Ping, He, Zheng, Chen, Xinyu, Li: Study on a surrounding rock pressure calculation method for super-large section highway tunnels. Symmetry11(9):1133.doi:10.3390/sym11091133 (2019).
10. Barton, N., Lien, T., Lunde, J.:Engineering classification of rock masses for the design of tunnel support. Rock Mechanics 6,189-236(1974)
11. Verman, M., Jethwa, J.L., Goel, R.K.: Estimation of wall support requirements for underground powerhouse cavern of Sardar Sarovar project in India. In: Proceeding international congress on options for tunnelling, Amsterdam, The Netherlands (1993).
12. Ramaswamy, N., Shah, B.J., Shah, K.N.: Sardar sarovar (Narmada project): geotechnical investigations for power house cavern. In: Proceeding international symposium on tunnelling for water resources and power projects, India,pp.59-64(1988).

13. Samadhiya, N.K., Viladkar, M.N., Bhargava, P.: Software package for 3-dimensional analysis of caverns. Journal of Rock Mechanics and Tunnelling Technology 10(1),49-76(2004).
14. Samadhiya, N.K.: Constitutive laws for jointed rock mass. Journal of Rock Mechanics and Tunnelling Technology 13(2),77-92 (2007).
15. Samadhiya, N.K., Viladkar, M.N., Moataz, A Al-Obaydi: Numerical implementation of anisotropic continuum model for rock masses. International Journal of Geomechanics, American Society of Civil Engineers 8(2),157-161(2008).
16. Samadhiya, N.K., Viladkar, M.N., Moataz A Al-Obaydi: 3-D joint/interface element for rough undulating major discontinuities in rock masses. International Journal of Geomechanics, American Society of Civil Engineers 8(6),327-335(2008).
17. Dasgupta, B., Lorig, L.J.: Numerical modelling of underground powerhouse in India. Journal of Rock Mechanics and Tunnelling Technology 2(2),119-134(1996).
18. Samadhiya, N.K., Viladkar, M.N., Singh, Bhawani: Three dimensional analysis of a powerhouse cavern in an anisotropic rock mass. International Journal of Rock Mechanics and Mining Sciences 41(3) SUPPL. 1:3B14, 1-6(2004).
19. Neville, A.M.: Properties of concrete. 3rd Ed. Longman Scientific and Technical an Imprint of Longman Group, UK(1981).
20. Divatia, E., Trivedi, V.P.: Special design features of right bank underground powerhouse complex. Indian Journal of Power and River Valley Development XL(9),261-269(1989).
21. Singh, B., Viladkar, M.N., Samadhiya, N.K., Sandeep: A Semi-empirical method for the design of support systems in underground openings. Tunnelling and Underground Space Technology 10(3),375–383(1995).
22. Bhasin, R., Singh, R., Dhawan, A.K., Sharma, V.M.: Geotechnical evaluation and review of remedial measures in limiting deformation in distressed zones in a powerhouse cavern. In: Proceeding international conference on design and construction of underground structures, pp.145 – 152, New Delhi India (1995).
23. Grimstad, E., Barton, N.: Updating of the Q - system for NMT. In: Proceeding international symposium on sprayed concrete - modern use of wet mix sprayed concrete for underground support, pp.46-66,Fagerenes (1993).
24. Barton, N.: Cavern design for Hong Kong rocks. In: Proceeding rock cavern seminar - Hong Kong, Institution of Mining & Metallurgy, 179 – 202, London (1989).
25. Jethwa, J.L., Goel, R.K., Verman, M., Singh, B.: A report on support requirements for Sardar Sarovar Powerhouse Cavern, Gujrat. CSIR-CIMFR, Dhanbad, India (1990).